Femtosecond Studies of Protein – DNA Binding and Dynamics: Histone I

Dongping Zhong, Samir Kumar Pal, and Ahmed H. Zewail*[a]

*In this contribution, we report studies of the nature of binding interactions and dynamics of protein histone I (H1) with ligands in solution and as a complex with DNA, an important biological process for the higher-order structure in chromatin. With femtosecond time resolution, we examined the role of solvation by water, the micropolarity at the interface of the binding site(s) of H1, and the rigidity of the complex structure. We used two biologically common fluorescent probes: 2-(*p*-toluidino)naphthalene-6-sulfonate (TNS) and 5-(dimethylamino)naphthalene-1-sulfonyl chloride (DC). By noncovalently attaching TNS and covalently adducting DC to the binding sites we found that the solvation dynamics, which occur within 1 ps, for the probe at the protein surface and in bulk solution are comparable, indicating the significant contribution of bulk water shells. However, the local polarity changes significantly, reflecting the change in dielectric properties at the protein/water interface. The binding structure of the protein – DNA complex was examined by the local orientational motion of the probe. The covalently bound DC molecule, sandwiched between the protein and DNA, was found to be frozen, revealing the very rigid structure at the recognition site, while, for noncovalently bound TNS, the complexes displace the probe. The dynamical rigidity of the complex, and the role of solvation and interface polarity, elucidate the strong recognition mechanism between DNA and the protein by electrostatic interactions, which are important to the compactness and to chromatin condensation in the biological function.*

KEYWORDS:

femtosecond dynamics · molecular recognition · protein – DNA interactions

Introduction

A wide variety of biological processes are controlled by the interactions between proteins and DNA.[1–3] The mechanism of binding must address the dynamics of recognition and the rigidity of the complex,[4] and the possible influence for the interaction with water near the binding site.[5] To understand these interactions at the local molecular scale, several questions need to be addressed. What is the time scale of solvent relaxation at the protein surface? What is the micropolarity near binding sites? How strong is the binding interaction and how rigid is the structure?

One class of protein – DNA systems is that involving histones (H). The complexes have an important biological function in chromatin condensation.[6] The primary structure of H1 has an uneven distribution of positively charged amino-acid residues along the polypeptide chain with three distinct domains.[7] The amino (N; ~30 residues) and the carboxyl (C; ~100 residues) termini are coiled randomly and contain a great number of positively charged lysine and arginine groups, while the central globular domain (~80 residues) consists of a three-helical bundle with a β-hairpin at the carboxyl terminus (Figure 1) and is less basic with the bulk of hydrophobic residues.[7b] In the binding interaction with DNA, the central globular moiety is partially participated whereas the two termini are mostly involved.[7c, 8, 9]

Extensive studies[6] of the artificial H1 – DNA complexes indicate that the strongest binding interaction is at the basic C-terminal tail of H1; the N-terminal binds to DNA less strongly. In nucleosome, the protein H1 seals two turns of the linker DNA by the main electrostatic binding around the nucleosomal core, where DNA complexes with each two of four core histones H4, H3, H2A, and H2B (Figure 1). In chromatin, the unique H1 – DNA complex and possibly the hydrophobic globular domain of H1 play an important role on forming a higher-order structure in chromatin condensation.[10]

In this study, we use two biologically common fluorescent probes, TNS and DC (Scheme 1; for fluorescence spectra see Figure 2) to examine the local molecular dynamics at the protein H1 surface and the rigidity of the binding structure. The anionic TNS, one of the most popular biological probes,[11–13] binds mainly with the positively charged basic residues on the two termini (C and N) by *noncovalent* electrostatic interactions; there is also the possibility for TNS to bind with the central globular domain by hydrophobic and electrostatic attractions.[7, 11] On the other hand, DC mainly binds by *covalent* adduction with α-amino group of the N-terminus and ε-amino groups of the two termini of H1.[14, 15]

Upon UV excitation, both probe molecules undergo a twisted intramolecular charge transfer (CT) reaction.[16–18] By observing the femtosecond to nanosecond dynamics of population and

[a] *Prof. A. H. Zewail, Dr. D. Zhong, Dr. S. K. Pal*
Laboratory for Molecular Sciences
Arthur Amos Noyes Laboratory of Chemical Physics
California Institute of Technology
Pasadena, CA 91125 (USA)
Fax: (+1) 626-7928456
E-mail: zewail@caltech.edu

polarization-analyzed anisotropy for the protein (H1) – ligand and the H1 – DNA complex, we elucidate the nature of local solvation and polarity at the protein surface and the binding structure of the complex. To "mimic" the surface effect of the H1 protein, which exhibits a positive charge distribution in contact with the water layer, we also studied the cationic micelles (Figure 1) probed with TNS; solvation, micropolarity, and the local rigidity were examined. The dynamics of both probes, TNS and DC, in polar solvents (water and methanol) were characterized for the first time with femtosecond time resolution in order to unravel the change in dynamics upon recognition by the micelle, protein, or protein – DNA complexes.

Experimental Section

All experiments were carried out by using the femtosecond-resolved fluorescence up-conversion technique. The experimental setup is described in detail elsewhere.[19] The fs pump pulse (250 nJ) from the tunable laser was used at 325 nm. The probe pulse was set at 790 nm. The fluorescence was collected by a pair of parabolic focus mirrors and sent into a nonlinear crystal to mix with the probe pulse. The up-converted signal in the deep UV range (210 – 330 nm) was detected by a photomultiplier after dispersion through a double-grating monochromator. Most transients were taken at the magic angle (54.7°) of the pump polarization, relative to that of the fluorescence (determined by the nonlinear crystal). For anisotropy

Editorial Advisory Board Member:[*] *Ahmed H. Zewail was born in Egypt on February 26, 1946. He received his B.S. and M.S. degrees from Alexandria University, and his Ph.D. from the University of Pennsylvania. After completion of his Ph.D. he went to the University of California, Berkeley, as an IBM research fellow. In 1976 he was appointed to the faculty at Caltech and in 1982 became a full professor. He is currently the first Linus Pauling Chair Professor of Chemistry and Professor of Physiscs at the California Institute of Technology, and Director of the NSF Laboratory for Molecular Sciences (LMS). His research interests center on the development of ultra-fast lasers and electrons for studies of dynamics in chemistry and biology. In the field of femtochemistry, developed at Caltech, fundamental femtosecond processes in chemistry, physics, and biology are investigated. His outstanding contributions have been widely recognised with numerous prestigious awards and honors including the Grand Collar of the Nile from President Murbarak, the Robert A. Welch Prize Award, the Benjamin Franklin Medal, and the Leonardo Da Vinci Award of Excellence. In 1998 Egypt issued a postage stamp with his portrait and in 1999 he received the Nobel Prize for Chemistry.*

[*] *Members of the Editorial Advisory Board will be introduced to the readers with their first manuscript.*

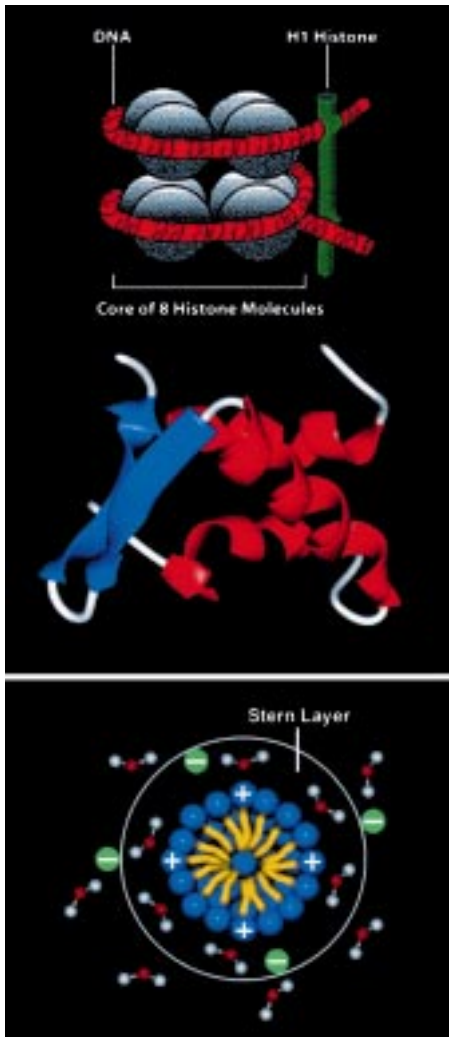

Figure 1. *Illustration of the core nucleosome particle structure with histone I sealing the two extremities of DNA (top). The structure of the globular domain in histone I is determined from NMR studies[7b] (middle). A schematic of cationic micelle structure[27b] (bottom).*

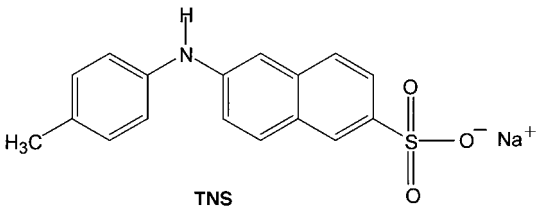

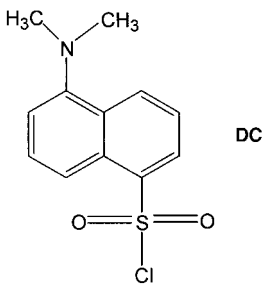

Scheme 1. *Molecular structures of TNS and DC.*

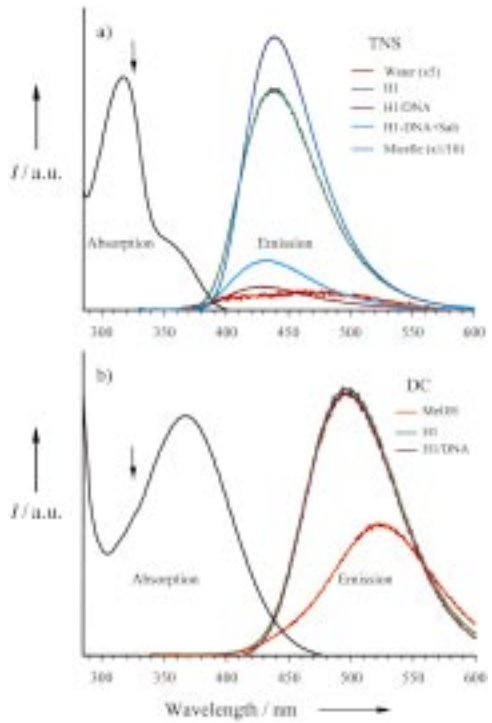

Figure 2. *The steady-state fluorescence spectra of the probes a) TNS and b) DC in chemical and biological environments studied with the same probe concentration. The absorption spectra are also shown and the arrows mark the excitation wavelength (325 nm). Note the huge enhancement in emission of TNS in H1 and the micelle.*

measurements, the pump polarization was adjusted to be parallel or perpendicular to that of the fluorescence, defining the anisotropy $r(t) = (I_{\parallel} - I_{\perp})/(I_{\parallel} + 2I_{\perp})$.

Sample preparation and properties: The protein calf thymus H1 (type III-SS), calf thymus DNA, and TNS were purchased from Sigma, DC from Molecular Probes, and CTAB from Fluka. All samples were used as received. Aqueous biological solutions were prepared in phosphate buffer (0.1 M, pH 7).

The TNS – H1 complexes were prepared by mixing of TNS (150 μM) with H1 (1 mg per 1 mL TNS solution) in a neutral buffer solution. The covalent attachment of DC to H1 (adduct formation) was achieved following the procedure from Molecular Probes. Briefly, DC was first dissolved in a small amount of dimethyl formamide and then injected into the sodium bicarbonate solution (0.1 M) of H1 (pH 8.3). The reaction was terminated by adding a small amount of freshly prepared hydroxylamine (1.5 M, pH 8.5) after incubating it for 1 h at 4 °C with continuous stirring. The solution was then dialysed exhaustively against phosphate buffer (0.1 M) to separate the adducts (DC – H1) from any unreacted DC and its hydrolysis product. It should be noted that DC – H1 complexes are quantitatively formed because of covalent synthesis, while for TNS – H1 the noncovalently bound complexes are ~92% at our TNS concentration on taking the equilibrium constant to be $\sim 10^6\ M^{-1}$.[12]

The yield of 92% complexes is obtained assuming, at least, a triple binding of TNS to H1 (1:1 binding gives ~33% complexes); the covalent adduction of DC to H1 also multiply binds[15] and adducts to the α-amino group at the N terminus first and then to ε-amino groups (lysine) in the protein H1. The multiple binding is expected because of the high charge density in protein domains. The positive charge distribution in the lysine-rich H1 protein is 30% of the total number of residues (~210), that is ~63 residues are positively charged. The distribution for these ~63 residues is as follows: ~44 in C-terminal, ~12 in globular, and ~7 in N-terminal. Thus, the positive charge-density distribution in each domain is about 42% (C-terminal), 16% (the globular domain), and 23% (N-terminal). Accordingly, multiple bindings between TNS and H1 are dominant at the terminal groups. Because of the three-dimensional order structure in the globular domain, compared to the random-coiled structure of termini, it is likely that the globular structure with its positive charges will be less effective in binding with DNA.

The H1 – DNA association procedure is similar to that of ref. [9]. Sodium chloride (1.2 M) and DNA (1 mg mL^{-1}) were dissolved in the TNS – H1 buffer solution by stirring. After 1 h, the solution was ready for association of the complex by the step dialysis method (2 h against 0.6 M NaCl, 2 h against 0.3 M NaCl, 4 h against 0.01 M, and finally 15 h against 1 mM NaCl). The buffer was phosphate (0.1 M, pH 7) in all cases. At the concentrations used, it is known[9] that DNA and H1 bind noncooperatively as DNA – H1 species and not as a precipitate of many such complexes. For the H1/DC/DNA system, DNA was dissolved in DC-labeled H1 solution with NaCl (1.2 M) and H1-DNA complexes were again prepared by the step dialysis. At the end of the association, all solutions were perfectly clear.

Steady-state optical studies: Upon the addition of H1 to an aqueous solution of TNS (see above) the fluorescence emission increases by ~60 times and the "maximum" shifts to the blue by 40 nm, from 470 nm in pure water to 430 nm (325 nm excitation); see Figure 2a. We then made the attachment of DNA to TNS/H1 solutions, maintaining the relative concentrations. The formation of H1 – DNA complexes (deoxyribonucleic protein, DNP) results in an 11-fold decrease in fluorescence, compared to that of H1 alone. The addition of sodium chloride (1.2 M) increases the fluorescence 2.5-fold, compared to DNP, and this change in ionic strength is known to cause the ionic dissociation of DNP.[9] The emission of TNS in bulk water has a quantum yield of ~0.001[13] and when measured in CTAB micelles we found the fluorescence to be ~670 times greater than in pure water.

DC is sparingly soluble in pure water but dissolves in methanol (MeOH). The emission maximum in MeOH lies at 510 nm and the emission quantum yield is estimated to be about 0.4.[20] When DC is covalently attached to H1 (DC – H1 adduct), compared to DC in MeOH at the same optical density, the fluorescence emission increases by about a factor of two. The spectrum is 25 nm blue shifted. However, the fluorescence intensity and profile remain unchanged when the adduct forms a complex with DNA, as shown in Figure 2b.

Results and Discussion

Ligand in Bulk Solvents: Dynamics of Solvation, Charge Separation, and Twisting

Figure 3a shows the femtosecond-resolved transients of TNS in pure water with a systematic series of wavelength detection. All transients show three distinct time scales. The signal initially decays at the blue side (410 – 470 nm) over 390 – 770 fs but rises at the red side (470 – 570 nm) over 190 – 680 fs. In contrast, on the picosecond time scale, the second component decays for all wavelengths detected with a time constant of 1.9 (410 nm), 2.6 (420nm), 3.2 (430 nm), 3.8 (470 nm), 5.8 (510 nm), and 10 ps (570 nm). The long-time component decays with a time constant of ~60 ps.

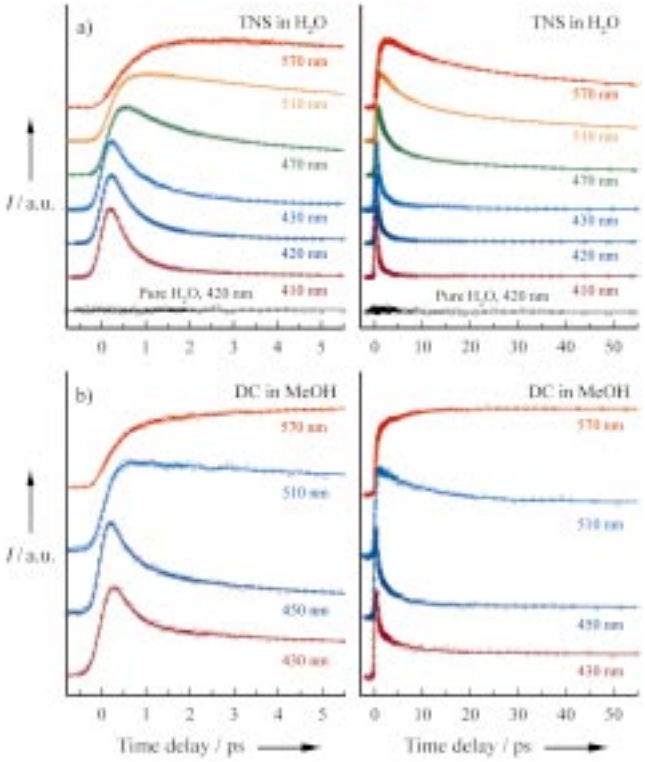

Figure 3. *Femtosecond-resolved transients a) of TNS in pure water and b) DC in MeOH with a series of wavelength detection shown for short (left) and long (right) time scales. The transients are normalized for comparison. The pure solvent signal, without the probes, is shown here for water at 420 nm. Note the difference of long-time component contributions for TNS and DC at the blue edge; see text.*

The initial femtosecond decay at the blue side and rise at the red side is a manifestation of solvation dynamics in water. This is because TNS, with its large dipole change upon excitation, lowers its potential energy as the water molecules solvate the probe ligand. By following the time-resolved emission (Stokes shift with time), we constructed the correlation function (solvent response function) in order to obtain the solvation time: $C(t) = [\nu(t) - \nu(\infty)]/[\nu(0) - \nu(\infty)]$, where $\nu(t)$, $\nu(0)$ and $\nu(\infty)$ are time-resolved emission maxima in units of cm^{-1} respectively. The average solvation time is $\sim$700 fs, consistent with the reported value for bulk water.[21, 22][**]

The observed picosecond component, which is always manifested as a decay, represents the twisting motion of TNS in a barrier crossing from the initial to the final state of charge separation. In the ground state, the two aromatic moieties have an angle of $\sim 50^\circ$. Upon the $^1\pi$-π^* excitation, charge flows from the donor phenyl ring to the acceptor naphthalene ring, facilitated by the conjugation of the lone-pair electrons at the nitrogen atom with the phenyl ring.[16] As the molecule twists toward the CT state, which is stabilized by the polar solvent, a perpendicular configuration of the two rings is reached.[17] The dynamics are pictured by a contour map of the free energy along the solvation and twisting coordinates, as shown in Figure 4a, and an energy diagram, in Figure 5a, to illustrate the barrier crossing process.

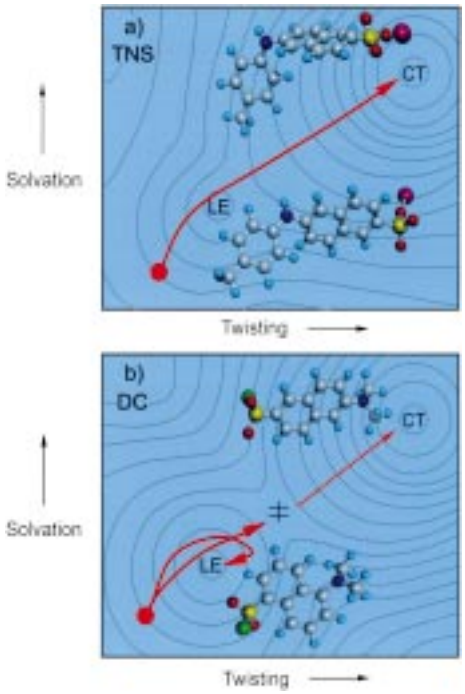

Figure 4. *A schematic of excited-state free energy contour map along the two coordinates involved, solvation and twisting, for a) TNS and b) DC. The corresponding molecular structures are also shown. The initial wave packet evolves along both twisting and solvation coordinates. For TNS, nearly all reaction trajectories end in the CT state while for DC a substantial number of molecules are trapped in the LE state.*

As solvation proceeds, the total available energy in the molecule above the twisting barrier decreases with time. The resulting twisting time becomes longer, consistent with the gradual increase in the decay time of the observed picosecond component from the blue side to the red side of the emission. Note that the time scale of the twisting (ps) is longer than that of solvation (fs). Thus, during the transformation from the initial, locally excited (LE) state to the CT state, the water solvent can "immediately" respond to the new configuration of the solute.

In a nonpolar solvent, the energy of CT moves up because of the lack of stabilization by the solvent. The lifetime of the LE state in an aprotic, nonpolar solvent was reported to be 7.3 ns with a maximum emission at 420 nm and a quantum yield of 0.3.[23] Since the crossing to the CT state occurs in a few picoseconds (the twisting barrier is relatively small), the observed long-time decay ($\sim$60 ps) is due to the emission of the CT state following the twisting. At the blue edge (410 – 430 nm), there is nearly no contribution from this long-time 60 ps component or any longer-time decay as the maximum contribution of such component(s) was $\sim$1 – 2%. The absence of the

[**] *The function C(t) for coumarin 343 in water[22] has an initial Gaussian-type component (frequency 38.5 $ps^{-1} \approx 25$ fs in time width, 48% of total amplitude) and two exponential decay components of 126 fs (20%) and 880 fs (35%). Our solvation here is concerned with up to 1 ps decay without fully resolving the initial $\sim$100 fs component. Accordingly, the blue and red sides of the emission, which have the similar dynamical time scale, reflect the diffusive ($\sim$800 fs) motion of water molecules.*

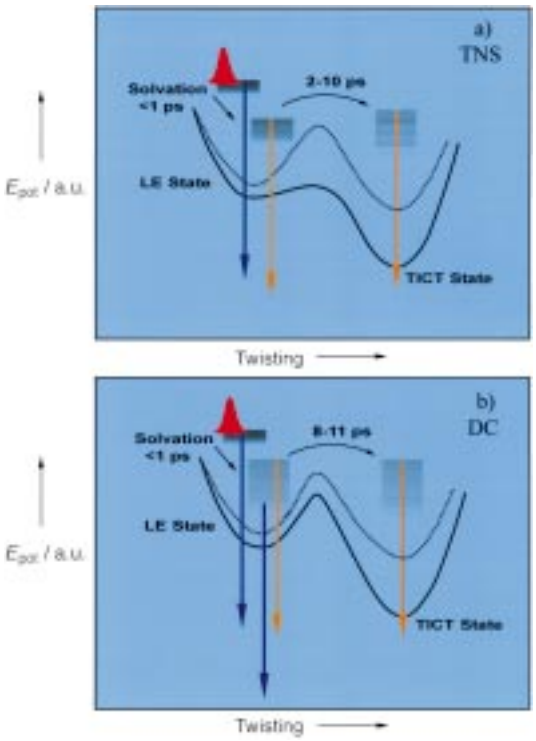

Figure 5. *Schematic potential energy curves along the reaction coordinate (twisting) for the two probes a) TNS and b) DC with the observed emission. The dashed lines present the potential energy curves when the probe binds to the protein H1. The barriers are increased mainly due to the lower micropolarity on binding sites. Note the nearly barrierless twisting motion for TNS in pure water.*

60 ps component in the blue emission further supports its origin from the CT, not the LE, state. Moreover, the absence of a significant long-time component in the blue emission indicates that the twisting is more effective than vibrational relaxation, which will lead to trapping in the LE state (Figure 4a and 5a), supporting the low-barrier picture.

At the red side, the observed long-decay signal ($\sim$60 ps) results from the CT-state emission. If this is the only process, then we expect a rise (a few picoseconds due to twisting) and a decay by $\sim$60 ps (lifetime). However, the transient signal in the red emission is a superposition of two contributions from the solvated LE state, mentioned above, and the twisted CT state (Figure 5a). The larger contribution of the decay signal from the solvated LE-state emission dominates the observed transient: a buildup of $\sim$700 fs by the solvation and a decay by the twisting, and a CT lifetime decay component. The rise component of the CT state is overwhelmed by the dominant, LE-state twisting decay component because the emission from both LE- and CT-states overlaps at the red side and the dynamical processes of both states, twisting decay and formation, occur on the same time scale. Note that vibrational relaxation must occur on a longer time scale than that of twisting, which is supported by the absence of a rising signal on the picosecond time scale at the red side. The extremely low quantum yield (0.001) in water[13, 22] indicates that the CT-state dynamics are dominated by non-radiative processes, for instance, the fast intersystem crossing as proposed in the literature.[24]

For the ligand DC, Figure 3b shows the transients in the polar solvent methanol (MeOH). The general mechanism of twisting is similar to that of TNS in water (Figures 4a and 5a). The solvation process dominates the initial ultrafast dynamics as observed in the distinct behavior of decay of the transients at the blue side and rise at the red side on the same femtosecond time scale; MeOH solvation is somewhat longer than water.[25] For the twisting motion across a barrier, we observed, in contrast with TNS, the LE-state decay at the blue-side emission and the CT-state buildup at the red-side emission, both with similar time constants of 8 – 11 ps. This observation indicates that the barrier of DC is relatively larger than that of TNS, consistent with the observation of a long-time decay component (25%) at the blue edge emission (430 nm) with a lifetime of $\sim$900 ps. This signal is from the trapped molecules in the LE state after solvation and below the twisting barrier (Figures 4b and 5b). The long-time decay component at the red side of emission (570 nm) is from the CT state and has a lifetime of $\sim$8 ns. The observed long lifetimes for both LE and CT states indicate that nonradiative processes in DC are not as efficient as in TNS, consistent with the large quantum yield of DC (0.4). The assignment of dual emission from the LE (at the blue edge) and CT states agrees with the reported fluorescence spectra in polar and nonpolar solvents,[18] namely a blue shift in nonpolar solvents.

Ligand – Protein (H1)/Micelles, Noncovalent Interactions

The transients of TNS in H1 solutions are shown in Figure 6 for three typical wavelengths (the blue-edge, peak, and red-tail emission). Following the methodology described above, we observed solvation to still occur on the femtosecond time scale and be similar to that in bulk water. This result is surprising given that the common picture for protein solvation is one in which the protein involves a water layer that is different from bulk water. However, if solvation is dominated by long-range water shells or involves networks of water structures then the $\sim$700 fs solvation time characteristic of bulk water is not surprising. Using the surface-sensitive second harmonic generation detection, Eisenthal's group has shown, that solvation at the air/water interface takes the same time as in bulk water.[26] It was concluded that solvation dynamics are dominated by the long-range solvent – solute interaction which extends from the second solvent shell to infinity. Our observation indicates that the rigid structure of water molecules[27] on the surface of the random-coiled termini does not play a significant role. Solvation in such rigid structures gives rise to dynamics on slower time scales and has recently been reported.[28–30]

The protein water "layer" is dominant in the hydrophobic globular domain and is used effectively to conserve the folded structures. The probe ligand interacts with the N and C termini by electrostatic interactions, as discussed above, but it should be noted that interactions between TNS and a hydrophobic group are also possible.[12] The electrostatic interaction of TNS with the terminal groups is supported by other observations. The addition of DNA to H1 – TNS complexes displaces the TNS molecules (Figure 2), and it is known that DNA binds to H1 mainly through N and C termini.[9] Furthermore, DC covalently

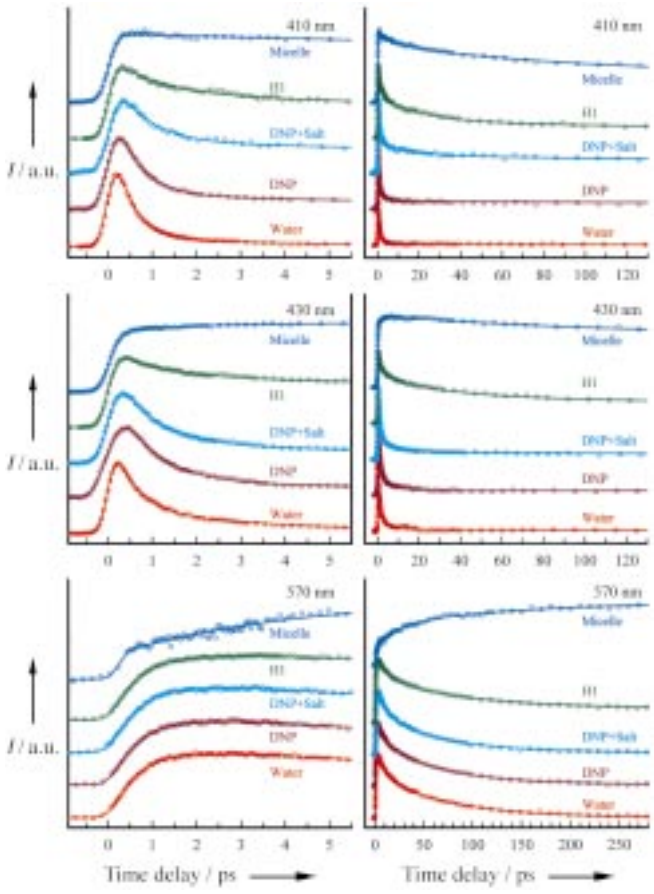

Figure 6. *The observed transients of TNS in water, the different biological environments studied, and in cationic micelles. Two time scales are shown, short (left) and long (right), for three typical fluorescent wavelengths: the blue-side, emission peak, and the red side. Note the change in time scale for the 570 nm case at long times. All transients are normalized for comparison.*

bound to H1 gives a similar solvation time; DC binds dominantly at the N and C termini (see below). The evidence of the TNS–hydrophobic interaction picture stems from the comparison of the steady-state emission in polar and nonpolar solvents, with the latter being similar in peak position to that in protein solution. However, as discussed below, the micropolarity near the interface between the ligand and the protein is determined by the combined dielectric constants of the two components.[31] In fact, the emission peak in protein solution is at 430 nm whereas in the less-polar solvent (THF) it is at 420 nm.

To mimic the cationic surface of H1, a chemical system of cetyltrimethyl ammonium bromide (CTAB) micelles was used. The interaction of TNS with the host occurs in the peripheral Stern layer (~10 Å) with the strong ion attraction on the inner shell. In this layer, the local polarity is greatly reduced and the effective viscosity is increased. The water molecules near the cationic shell become "rigid".[27b] As mentioned above, upon the inclusion of TNS in the micelle, the fluorescence emission increases by ~670 times. The transients become dramatically different from TNS in protein solution (Figure 6). We observed a much different solvation time scale: Solvation dynamics occur in hundreds of picoseconds, with a minor component of several picoseconds decay. This solvation behavior is expected because of the rigid structure of water molecules in the peripheral Stern layer.[32]

The micropolarity was probed by the twisting motion of the ligand which takes longer times in proteins than in water: 3.5 (410 nm), 9 (430 nm, emission peak), 10.5 (470 nm), 14 (510 nm), and 15 ps (570 nm). This lengthening reflects the increase in the effective twisting barrier in the protein environment. The long-time components (100 ps or longer) are greatly enhanced, consistent with a substantial trapping of molecules in the LE state (following solvation) due to the increase in barrier height. The observed huge enhancement of the steady-state fluorescence emission (Figure 2a), therefore, results from the trapping of the molecules in the LE state (Figure 5a). The CT state near the protein site must increase its energy in order for this trapping to be efficient; CT nonradiative decay also decreases as the CT shifts to higher energy. Accordingly, the effective dielectric constant must be smaller than that of bulk water. At an interface, the ligand molecule experiences the polarity from both sides[31] and the net local polarity is lower than that of the bulk. The increase in the barrier energy is dominated by the polarity effect (higher CT energy). This is evidenced by the similarity in time scales for the fraction of the molecules which undergo twisting above the barrier (25%, 10 ps).

The restriction on the twisting motion of TNS by the protein H1 is not significant because TNS interacts interfacially and not housed in the rigid protein pocket.[4] This is further supported by measurements of the local motion of the ligand (see below). In the micelle, no twisting motion was observed and all molecules are trapped in the LE state. The lifetimes increase to tens of nanoseconds, and emission becomes 670 times stronger. These results indicate that charge separation and twisting motion do not occur in the excited state because of the lower dielectric constant and the high microviscosity in the layer of the micelle.

To probe the local rigidity of ligand–protein complex, we measured the time-resolved anisotropy of TNS at the peak emission of 430 nm, shown in Figure 7a. It has three decay components: The major contribution (~75%) of the anisotropy decays with ~75 ps time constant and the final anisotropy is close to zero (0.015); the initial drop of the minor contribution occurs on the time scale of solvation and twisting. Because of its similarity to other anisotropy decays, the ~75 ps decay represents the diffusive motion of TNS at the terminal surface. Apparently, the electrostatic attraction does not place a significant restriction on the orientational motion of TNS, again consistent with the idea that it is not in a complete rigid layer. The picture envisaged is that the TNS molecule is labile on the H1 surface with the negative charge pointing to the cationic termini.

In contrast, the anisotropy of TNS in the micelle is persistent, as shown in Figure 7a. It has a single exponential decay of ~800 ps, a long orientation relaxation process. This significant increase in the relaxation time is due to the large rigidity in the Stern layer.[31] The fact that the anisotropy did not decay to zero, up to 500 ps, elucidates the rigidity of the entire molecule toward rotations. The lack of a 2 picosecond decay is consistent

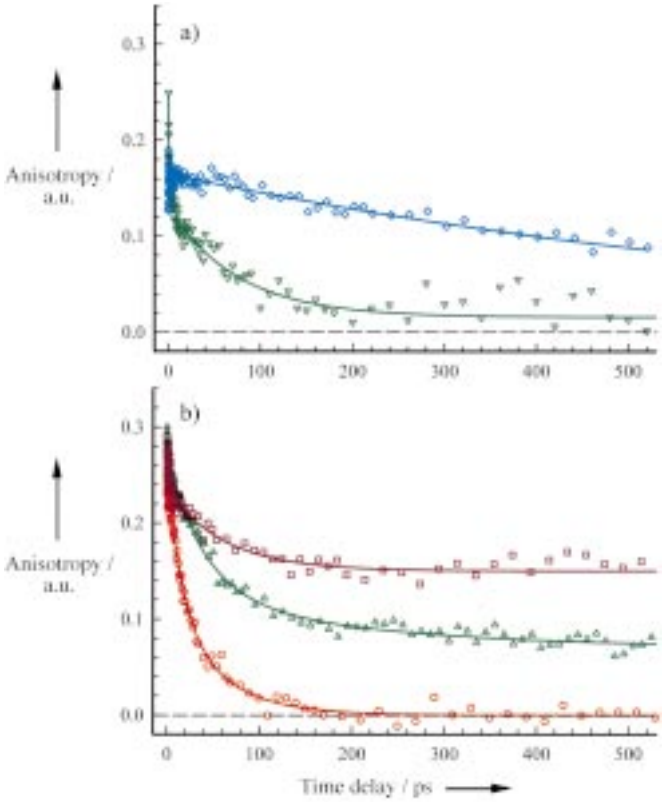

Figure 7. Femtosecond-resolved fluorescence anisotropy in different environments for a) TNS (◇ micelle, ▽ H1) and b) DC (□ DNP, △ H1, ○ MeOH) at the peak emission. Note the dramatic change for DC on going from free solvent MeOH to the protein H1 and to DNP.

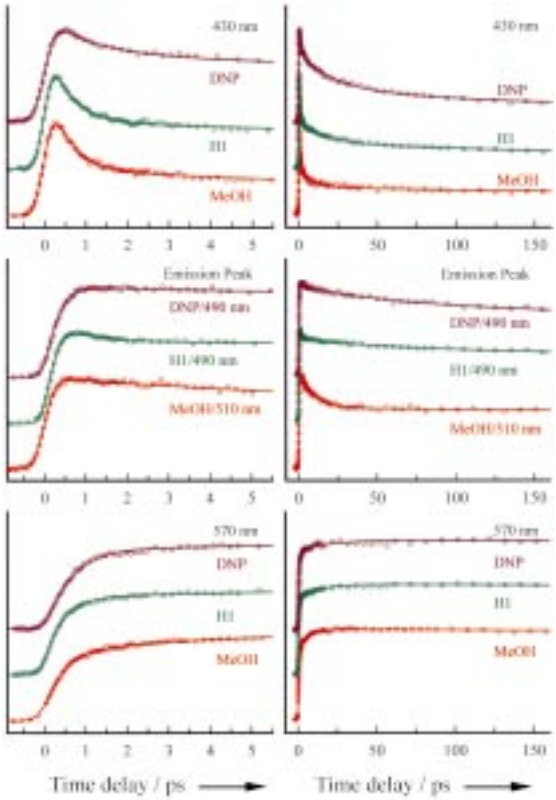

Figure 8. The observed transients of DC in MeOH and the different biological environments studied. Two time scales are shown, short (left) and long (right), for three typical fluorescent wavelengths: the blue-side, emission peak, and the red side. Note the difference of transients for H1 and DNP, even though both have the same fluorescence emission (Figure 2b). All transients are normalized for comparison.

with the hindrance of the intramolecular twisting motion; only the slow solvation dynamics in the LE state proceeds.

Ligand – Protein (H1) Covalent Adduction

To further characterize the two termini of H1 and its interaction with DNA in situ, we studied the covalent adduction of DC with H1. The transients of the DC – H1 adducts in water (with buffer) are shown in Figure 8 for three typical wavelengths. We observed similar dynamics and mechanism to that in bulk MeOH (Figure 4b and 5b). We did not observe noticeable changes in the solvation dynamics on going from bulk to protein solutions, as also in the case of TNS/H1 system. This result is convincing because neutral DC is covalently connected to the protein binding sites. Similar to TNS in H1 solution, the twisting motion takes a longer time: 16 ps at 430 nm and 48 ps at 490 nm, which is due to the increase of the twisting barrier. The fluorescence emission is blue shifted by ~20 nm and the quantum yield increases by a factor of two. These results again reveal the lower micropolarity at the interface of protein termini and water. Note that the increase in quantum yield for DC is not as large as for TNS because of the trapping of DC molecules in the LE state (Figure 5b) and its large quantum yield (0.4) in bulk solvents.

The anisotropy of DC is shown in Figure 7b, together with that of DC in free MeOH for a comparison. In MeOH, the two major decay components have time constants of 14 (40%) and 50 ps (50%), except for a small initial decay (~10%) which corresponds to the structure relaxation from ultrafast solvation. The 14 ps decay is similarly due to the twisting motion. The time constant and percentage contribution are in good agreement with those observed at the magic angle. The second component (50 ps) represents the orientation relaxation of DC. According to the Stokes-Einstein-Debye hydrodynamics theory and assuming a prolate shape of the molecule,[33, 34] the rotational relaxation times should be 106 ps and 36 ps under stick and slip limits, respectively. Our measured value of 50 ps is toward the slip limit.

When DC is covalently connected to H1, the measured anisotropy dramatically changes and the time constants of the two major decay components increase to 40 and 207 ps. The anisotropy does not decay to zero, up to 500 ps. Both the twisting motion and the orientation relaxation slow down by a factor of about four. The increase of the orientation relaxation time is due to the covalent anchoring of DC to the H1 surface, which restricts the motion by the H1 backbone. The anisotropy due to the orientation relaxation (207 ps) decreases from 0.13 to the final value of 0.07. This change corresponds to an orientational motion in a cone with an estimated angle of ~20°, reflecting a very restricted local motion. The whole DC – H1 complex relaxes on a much longer time scale.

Protein (H1) – DNA Binding

After complexation of TNS/H1 with DNA to form DNP, the fluorescence emission decreases considerably, by a factor of ~11 (Figure 2a). The transients are shown in Figure 6 and are similar to those observed in bulk water (Figure 3a). Because DNA and the TNS mainly bind to C and N termini of H1, the results indicate that DNA repels TNS out of the binding sites into the water solution. Thus, the "surface – surface" electrostatic interaction between DNA and the protein H1 is much stronger than the "point-surface" contact of TNS with H1. A small percentage of a long-time decay (~500 ps) component was observed for all wavelengths (Figure 6). In addition, the fluorescence profile is similar to that of TNS in the protein H1 (Figure 2a). Thus, this small fraction of TNS molecules (~10%) left on the H1 surface probably reflects the hydrophobic binding interaction of TNS with the globular domain of H1.

We also conducted experiments at high salt concentrations. By adding salt (1.2 M NaCl) into the DNP solution, it was expected that DNA dissociates from the protein with the possibility of TNS binding back to H1.[9] However, we observed that the fluorescence emission only increases by a factor of 2.5 (Figure 2a), indicating that only ~17% of TNS molecules from water binds back to the protein H1. This observation suggests that DNA, because of its proximity to the protein, prevents a significant fraction of TNS molecules in water from binding back to the termini. The transients remain similar as in DNP except for the increase of the long-time decay contribution at the blue edge (410 nm at Figure 6). The appearance of DNA near H1 increases the microviscosity of the TNS – H1 environment and hence the increase of the twisting barrier. Consequently, most of the reassociated TNS molecules are trapped in the LE state, consistent with the observed increase of the long-time components (only) at the blue side.

DNA forms complexes[8, 9] with DC – H1 and the structure is expected to be sandwich-like (see Figure 9). Although the steady-state fluorescence emission shows *no* change (Figure 2b), the transients are different (Figure 8). The solvation process becomes somewhat slower. For example, at 430 nm the initial component of DC decays with a time constant of 600 fs in H1 (62%) and increases to 1.4 ps (30%) in DNP solutions. The twisting motion also takes a longer time of 22 ps and the percentage contribution grows from 18% in H1 to 40% in DNP solutions. These results indicate that the H1 – DNA binding reduces the number of water molecules accessible to the protein surface, resulting in the increase of the local effective viscosity and the decrease of the local polarity.

The local motion of DC directly probes the binding rigidity of DNA with H1. After complexation with DNA, the anisotropy, shown in Figure 7b, is persistent up to 500 ps with a large constant value of 0.15. The early decay component of 62 ps results from the structural changes by the intramolecular twisting motion, as also observed at the magic angle. The persistent of the anisotropy is very striking, indicating that no local orientational motion was observed and DC is essentially "frozen" after DNA binds to H1. These findings indicate that the binding interaction of H1 – DNA is relatively strong and the local structure is very rigid.

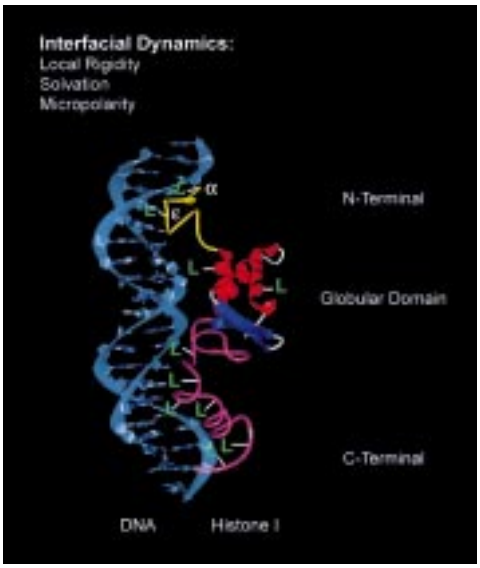

Figure 9. *Model of the interaction between the protein H1 and DNA, showing the interfacial dynamics studied through the covalent and noncovalent labeling of ligands ($\mathscr{L}$ and L) to the protein. $\mathscr{L}$ is a ligand reacting with the α-amino group at the N-terminus: For the DC ligand this means $\mathscr{L} \equiv D$, and the covalent binding results from the reaction $NH_3^+{-}P + DC \rightarrow NH_2^+D{-}P + HCl$, where P is the polypeptide chain. L is a ligand reacting with the ε-amino groups in lysine of the protein, that is, $L \equiv D$. The reaction is $R{-}NH_3^+ + DC \rightarrow R{-}NH_2^+D + HCl$, where R is the remaining lysine residue, connected to the polypeptide chain. The distribution of lysine through the protein H1 is dominated at the termini with the charge-density distribution discussed in text.*

Conclusion

Studies of femtosecond dynamics of ligand probes (TNS and DC) with the protein histone I and its DNA complexes elucidate the nature of the recognition process and the key time scales involved for complex rigidity, solvation, and micropolarity. These studies attempt to link structural and dynamical features for insight into the biological function of nucleosome formation and chromatin condensation.

The rigidity of the protein – DNA complex was measured using the time-resolved anisotropy which probes orientational motions of the ligand DC covalently adducted to the binding sites of the protein histone I. The anisotropy persists for more than 500 ps, in contrast to the behavior in the abscence of DNA (200 ps) or in liquid methanol (50 ps). These results indicate the suppression of ligand motion in the complex; without DNA binding, the ligand experiences a motion in a cone with an angle of ~20°. This relatively strong binding is also evident in the studies we made for the other ligand, TNS, which binds noncovalently to the protein. With DNA, the ligand is displaced (90%) elucidating the stronger recognition of protein/DNA relative to that of protein/TNS. The highly rigid H1 – DNA complex and the strong binding in the recognition of DNA by the protein H1 are perhaps key features in the sealing of the linker DNA during the nucleosome formation.

Solvation dynamics at the binding sites were measured from the solvent response function as probed by the temporal behavior of ligand during solvation (dynamical Stokes shift). The solvation process of DC or TNS/protein occurs as fast as in bulk solvents, less than 1 ps, indicating the minor role of rigid water structures in the binding sites. This finding is significant for the recognition of DNA by the protein H1. Because the N and C termini, with relatively high densities of positive charges, are involved in the recognition by electrostatic interactions, these random coils optimize the attraction by utilizing labile bulk water, unlike the structural water layer needed around the globular domain to maintain a 3D hydrophobic structure. Interestingly, for TNS in micelles we do observe the effect of rigid water structure, both in the lengthening of solvation and orientational relaxation times. In the presence of DNA with DC – H1, solvation time is somewhat increased and we attribute such change to the proximity effect.

The micropolarity at the binding sites was detected by the change of the twisting motion of the ligands, which ultimately leads to charge separation. The twisting barrier is polarity sensitive but the local viscosity is not as influential, as evidenced by the similarity of solvation time for the protein and bulk water systems and by the measured anisotropy. For the protein H1, the barrier increases and the twisting time lengthens for both ligands. The observed lower micropolarity at the binding sites reflects an interfacial property which signifies the combined dielectric properties of the protein and bulk water. This finding may have an implication to the formation of an order structure (induced α-helix[35]) when the randomly coiled C-terminal binds to DNA. The overall picture which emerges is depicted in Figure 9.

This work is supported by the National Science Foundation. We would like to thank Dr. Chaozhi Wan for his help.

[1] T. K. Kim, R. H. Ebright, D. Reinberg, *Science* **2000**, *288*, 1418 – 1421.
[2] A. K. Mapp, A. Z. Ansari, M. Ptashne, P. B. Dervan, *Proc. Natl. Acad. Sci. USA* **2000**, *97*, 3930 – 3935.
[3] J. J. Li, X. Fang, S. M. Schuster, W. Tan, *Angew. Chem.* **2000**, *112*, 1091 – 1094; *Angew. Chem. Int. Ed.* **2000**, *39*, 1049 – 1052.
[4] D. Zhong, A. Douhal, A. H. Zewail, *Proc. Natl. Acda. Sci. USA* **2000**, *97*, 14056 – 14061.
[5] J. Higo, H. Kono, H. Nakamura, A. Sarai, *Proteins* **2000**, *40*, 193 – 206.
[6] J. Zlatanova, J. Yaneva, *DNA Cell Biol.* **1991**, *10*, 239 – 248.
[7] a) J. Allan, P. G. Hartman, C. Crane-Robinson, F. X. Aviles, *Nature* **1980**, *288*, 675 – 679; b) C. Cerf, G. Lippens, S. Muyldermans, A. Segers, V. Ramakrishnan, S. J. Wodak, K. Hallenga, L. Wyns, *Biochemistry* **1993**, *32*, 11345 – 11351; c) V. Ramakrishnan, *Curr. Opin. Struct. Biol.* **1994**, *4*, 44 – 50, and references therein.
[8] E. M. Bradbury, B. G. Carpenter, H. W. E. Rattle, *Nature* **1973**, *241*, 123 – 125.
[9] J. J. Lawrence, L. Berne, J. L. Ouvrier-Buffet, L. Piette, *Eur. J. Biochem.* **1980**, *107*, 263 – 269.
[10] J. Widom, *Annu. Rev. Biophys. Biophys. Chem.* **1989**, *18*, 365 – 395.
[11] W. O. McClure, G. M. Edelman, *Biochemistry* **1966**, *5*, 1908 – 1919.
[12] R. Wang, F. V. Bright, *Appl. Spectrosc.* **1993**, *47*, 792 – 799.
[13] A. Datta, D. Mandal, S. K. Pal, D. Das, K. Bhattacharyya, *J. Chem. Soc. Faraday Trans.* **1998**, *94*, 3471 – 3475.
[14] M. Nakabayashi, K. Mihashi, *Photochem. Photobiol.* **1981**, *33*, 449 – 453.
[15] *Handbook of Fluorescent Probes and Research Chemicals*, 7th ed. (Ed.: R. P. Haugland), Molecular Probes, Eugene, OR, **1999**, p. 12.
[16] E. M. Kosower, *J. Am. Chem. Soc.* **1985**, *107*, 1114 – 1118.
[17] K. K. Karukstis, D. A. Krekel, D. A. Weinberger, R. A. Bittker, N. R. Naito, S. H. Bloch, *J. Phys. Chem.* **1995**, *99*, 449 – 453.
[18] B. Ren, F. Gao, Z. Tong, Y. Yan, *Chem. Phys. Lett.* **1999**, *307*, 55 – 61.
[19] T. Fiebig, C. Wan, S. O. Kelly, J. K. Barton, A. H. Zewail, *Proc. Natl. Acad. Sci. USA* **1999**, *96*, 1187 – 1192.
[20] Y. H. Li, L. M. Chan, L. Tyer, R. T. Moody, C. M. Himel, D. M. Hercules, *J. Am. Chem. Soc.* **1975**, *97*, 3118 – 3126.
[21] W. Jarzeba, G. C. Walker, A. E. Johnson, M. Kahlow, P. F. Barbara, *J. Phys. Chem.* **1988**, *92*, 7039 – 7041.
[22] R. Jimenez, G. R. Fleming, P. V. Kumar, M. Maroncelli, *Nature* **1994**, *369*, 471 – 473.
[23] N. Sarkar, K. Das, S. Das, A. Datta, R. Dutta, K. Bhattacharyya, *J. Chem. Soc. Faraday Trans.* **1996**, *92*, 3097 – 3099.
[24] T. L. Chang, H. C. Cheung, *Chem. Phys. Lett.* **1990**, *173*, 343 – 348.
[25] T. Gustavsson, G. Baldacchino, J. C. Mialocq, S. Pommeret, *Chem. Phys. Lett.* **1995**, *236*, 587 – 594.
[26] D. Zimdars, J. I. Dadap, K. B. Eisenthal, T. F. Heinz, *Chem. Phys. Lett.* **1999**, *301*, 112 – 120.
[27] a) R. Pethig in *Protein – Solvent Interactions*, (Ed.: R. B. Gregory), Marcel Dekker, New York, NY, **1995**, pp. 265 – 288; b) N. Nandi, K. Bhattacharyya, B. Bagchi, *Chem. Rev.* **2000**, *100*, 2013 – 2045.
[28] B. J. Homoelle, M. D. Edington, W. M. Diffey, W. F. Beck, *J. Phys. Chem. B* **1998**, *102*, 3044 – 3052.
[29] X. J. Jordanides, M. J. Lang, X. Song, G. R. Fleming, *J. Phys. Chem. B* **1999**, *103*, 7995 – 8005.
[30] P. Changenet-Barret, C. T. Choma, E. F. Gooding, W. F. DeGrado, R. M. Hochstrasser, *J. Phys. Chem. B* **2000**, *104*, 9322 – 9329.
[31] H. Wang, E. Borguet, K. B. Eisenthal, *J. Phys. Chem. A* **1997**, *101*, 713 – 718.
[32] S. K. Pal, D. Sakul, D. Mandal, S. Sen, K. Bhattacharyya, *Chem. Phys. Lett.* **2000**, *327*, 91 – 96.
[33] C. Hu, R. Zwanzig, *J. Chem. Phys.* **1974**, *60*, 4354 – 4357.
[34] J. S. Baskin, M. Chachisvilis, M. Gupta, A. H. Zewail, *J. Phys. Chem. A* **1998**, *102*, 4158 – 4171.
[35] D. J. Clark, C. S. Hill, S. R. Martin, J. O. Thomas, *EMBO J.* **1988**, *7*, 69 – 75.

Received: November 30, 2000 [F 157]